Published in final edited form as:
Angew Chem Int Ed Engl. 2011 February 18; 50(8): 1922–1925. doi:10.1002/anie.201006579.

Synthesis and *In Vivo* Imaging of a ^{18}F-Labeled PARP1 Inhibitor Using a Bioorthogonal Scavenger-Assisted High Performance Method

Thomas Reiner, **Edmund J. Keliher**, **Sarah Earley**, **Brett Marinelli**, and **Ralph Weissleder**

Abstract

Pedal to the metal: Using inverse Diels-Alder catalyst free TCO/Tz cycloadditions, we were able to quickly and selectively generate an ^{18}F-labeled AZD2281-derivative from multiple different scaffolds (A–E). Excess cold material was removed within minutes using a TCO scavenger resin. This protocol allows the parallel synthesis of a library of potential PET imaging agents in a short time, increasing the efficiency of lead compound detection. The novel PET probe was successfully tested in biological assays and its potency and targeted accumulation was confirmed *in vivo*.

Keywords

PARP1; cancer; bioorthogonal conjugation; ^{18}F PET; *in vivo* imaging; scavenger resin

Poly-ADP-ribose-polymerases (PARP) and breast cancer susceptibility proteins (BRCA) are proteins that repair DNA breaks that occur during each cell cycle, and which must be repaired for a cell to survive. PARP repairs single-strand breaks and BRCA repairs double-strand breaks. In the absence of functional BRCA (e.g. when BRCA is mutated), PARP will repair both types of DNA breaks. Thus, PARP inhibitors (PARPi) are emerging as a useful therapeutic option (single agent or in combination with cytotoxic drugs), particularly for BRCA negative tumors.[1] Several small molecule PARP1i have been developed (e.g. olaparib/AZD2281, BSI101, AG014699, MK4827) and some of them are in clinical trials.[1–3] One problem in the assessment of therapeutic efficacy has been the inability to image PARP1 non-invasively at the whole body level and to quantitate therapeutic inhibition. Such a technology would also enable stratification of patients into appropriate treatment groups and to detect emerging resistance.[4] The design of PARP1 imaging agents - similar as with most other intracellular imaging agents - is complex and time-consuming, and iterative designs are often required to develop suitable compounds.

Given the emerging importance of PET imaging in preclinical and clinical settings[5–9] and evidence that fluorescently labeled PARP1-inhibitors could be used for cellular imaging,[10] we became interested in developing ^{18}F-labeled probes for whole body PARP1 imaging. Such radio-tracers could be particularly useful for measuring target inhibition of emerging therapeutic PARP1 inhibitors. Fluorinating native AZD2281 (Figure 1D) at the 2-fluorobenzamide position has been challenging because of the fluorine's inaccessibility. In addition, modifications based on tosylation and subsequent fluorination of the piperazine moiety is inefficient or results in decomposition of materials.[11] Furthermore, not all labeled high affinity ligands identified in cell screens will exhibit ideal pharmacokinetics (blood half-life, tissue distribution, excretion) for positron emission tomography (PET) imaging.

Correspondence to: Ralph Weissleder.

One way to identify useful imaging agents is therefore to empirically test a battery of different agents *in vivo*. This approach, however, places considerable demands on the labeling chemistry for each compound. First, fluorination has to be optimized for every single compound and the desired reaction products have to be separated as not to inhibit the target by co-injection of cold precursors. Labeling and separation are usually performed using automated units in enclosed lead shields under time constraints, given the short half-life of ^{18}F (109.8 min). Given these lengthy sequential optimization procedures for each individual compound, it would be tremendously useful to develop more facile and simple platform technologies to advance the development of imaging agents through high throughput synthesis and subsequent multiplexed *in vivo* testing. Here we describe one such approach based on the combination of (4+2) inverse electron-demand Diels-Alder cycloadditions and show its utility for the development of novel PARP1 PET imaging agents.

The (4+2) cycloaddition between *trans*-cyclooctene (TCO) and tetrazine (Tz) is a highly useful chemically orthogonal strategy[12–14] given the a) fast reaction times in excess of 6,000 $M^{-1}s^{-1}$, b) high selectivity, c) no need for elevated temperatures or catalysts, d) biocompatible reaction conditions, e) tolerance towards blood, serum and a wide variety of organic solvents and f) the availability of activatable tetrazinedyes.[14–18] In addition, the (4+2) Diels-Alder reaction is irreversible, stable and very fast. Despite the advantages and potentially broad utility of the (4+2) cycloaddition chemistries, there is currently little data on the biological behavior of dihydropyridazine and pyridazine linkers, how these linkers affect the affinity of small molecules for their targets, modulation of *in vivo* pharmacokinetics by the conjugate or whether this generic strategy could be used for *in vivo* PET imaging. Here we develop a generic platform for parallel radio-fluorination of small molecule inhibitors and show how labeled reaction products can be rapidly isolated for subsequent *in vivo* testing before ^{18}F decays. We characterize TCO/Tz-generated ^{18}F-AZD2281 conjugates and perform biological and *in vivo* experiments. We show that one lead compound allows whole body imaging of PARP-1 and is useful for quantitating PARP1 inhibition *in vivo*. These results should pave the way for more extensive use of the (4+2) cycloaddition for the development of PET imaging agents.

Radiolabeled AZD2281-derivatives were designed on the basis of *trans*-cyclooctene reactive tetrazines, which were covalently attached at the piperazine-position of AZD2281. We previously showed, that attachment of substituents to this position only minimally perturbs the ability of resulting AZD2281-derivatives to inhibit PARP1 activity.[10,11] One problem during the synthesis of ^{18}F-radiolabeled compounds is that in most cases large amounts of cold radiolabel-precursors have to be used to efficiently react small quantities of ^{18}F. The resulting mixtures are typically subjected to HPLC-purification to remove the excess cold starting material, which in most cases will compete with the radiolabeled probe for the targeted binding sites. To avoid lengthy HPLC-purifications, we designed a *trans*-cyclooctene resin, which was used to “pull out” excess tetrazine-conjugated AZD2281-derivatives from the reaction solutions (Figure 1A). The resin was designed from commercially available magnetic amine-decorated beads, which were reacted in a solution of DMF/PBS with a 75 mM solution of *trans*-cyclooctene NHS-activated carbonate **1** (Figure 1B). Loading of 13 μmol/g of the resulting TCO-decorated beads was determined using tetrazine-labeled Oregon Green-Tz,[16] whose absorbance at 504 nm was observed to measure the quantity of material pulled out of solution by the beads (see supplementary information for detailed descriptions).

Chemically orthogonal reactive radiolabeled ^{18}F-TCO **3** was synthesized by nucleophilic substitution of the tosylate of *trans*-cyclooctene **2** by $^{18}F^{-}$ in the presence of tetrabutylammonium bicarbonate (TBAB) (Figure 1C).[11] AZD2281-Tz **5** was synthesized

similar to procedures recently described.[10] For ^{18}F-AZD2281 **6**, **3** and **5** were combined in a mixture of H_2O and DMSO (1000 μCi and 130 nmol, respectively) and stirred vigorously for 3 min.

This results in quantitative conversion of ^{18}F-TCO **3**, yielding a mixture of ^{18}F-AZD2281 **6** and excess AZD2281-Tz. Subsequently, treatment of this solution for 5 min with the TCO-decorated scavenger resin (4 mol eq. of TCO) removed unreacted AZD2281-Tz with minimal loss (approx. 4%) of radio-labeled compound **6**. Magnetic removal of the beads provided **6** in 92.1 ± 0.4% dcRCY and reconstituted in medium suitable for animal injection (Figure 1A and 1E). HPLC-analysis of the reaction mixture before and after treatment with the TCO-decorated scavenger resin shows that the absorption-peak, resulting from AZD2281-Tz, completely vanishes, whereas the activity-peak, resulting from ^{18}F-AZD2281, persists (Figure 1F).

The IC_{50}-value of 18F-AZD2281 **6** against PARP1 was determined to be 17.9 ± 1.1 nM in biochemical essays using the isolated enzyme (AZD2281 itself has an IC_{50} of 5 nM).[11,19,20] This makes PARP1 an ideal target for rapid screening of ^{18}F-labeled inhibitors, as it can accommodate relatively large prosthetic groups that do not affect binding affinity. To determine the inhibitor's performance in cell based *in vitro* essays, MDA-MB-436 and MDA-MB-231 cells were plated (5×10^5 cells/well) and incubated at 37 °C over night. Subsequently, both cell lines were incubated with either 5 μCi of ^{18}F-AZD2281 or a mixture of 5 μCi of ^{18}F-AZD2281 and AZD2281 (final concentration AZD2281: 1 μM). Cellular uptake of ^{18}F-AZD2281 was determined by quantification of the remaining activity after incubation and washing of the adherent cells. ^{18}F-AZD2281 was shown to be cell permeable and its uptake inhibitable upon addition of excess non-radioactive AZD2281 (Figure 2). Uptake of ^{18}F-AZD2281 was lower for MDA-MB-231 cells as compared to MDA-MB-436 cells, which correlates with protein expression of PARP1 in the respective cell lines (see supplementary information for details).

For subsequent *in vivo* experiments, 30 μCi of ^{18}F-AZD2281 were injected into Nu/Nu mice and imaged via PET/CT over 2h time. Figure 3A displays the probe's distribution at 10, 30 and 50 minutes. Images clearly show initial localization (10 min) of the probe to be mainly in liver, gall bladder and intestines, consistent with hepatobiliary excretion. After 50 min (Figure 3A), the majority of the probe left the bloodstream ($t_{1/2}$ = 6 min) and was excreted via the large intestines.

Tumor-bearing mice were obtained by injection of MDA-MB-436 (5×10^6 cells in matrigel) cells into the flanks of Nu/Nu mice and the tumors allowed to grow and vascularize for 7 days. Figure 3B shows a three-dimensional reconstruction of a tumor bearing mouse injected with 30 μCi of ^{18}F-AZD2281.

Uptake in the tumors is clearly visible. Immediately after imaging, mice were treated with 1 mg AZD2281 BID (*ip*). Re-injection of 30 μCi of ^{18}F-AZD2281 confirmed inhibition of the probe's uptake into the tumors (Figure 3B and 3C). Therefore, due to the rapid decay rate of ^{18}F, each mouse serves as its own control on subsequent days of imaging, facilitating direct comparisons of SUV.

In summary, we show that a) ^{18}F-AZD2281 accumulates in PARP1 over-expressing cancer cells (e.g. MDA-MB-436), b) that the cellular accumulation can be inhibited by cold AZD2281, c) that ^{18}F-AZD2281 accumulates in PARP-1 mouse models of cancer *in vivo*, d) that PARP-1 inhibition can be quantitated via PET imaging *in vivo.* The imaging agent was developed in relatively short time using the above described chemically orthogonal scavenger-assisted high performance method. Scavenger beads for alternative conjugation

methods could also be developed and applied in similar ways. However, we believe that the described method is particularly appealing for development of PET imaging agents because the extremely fast kinetics of the tetrazine/*trans*-cyclooctene inverse electron-demand Diels-Alder reaction at room temperature, its independency of catalysts and high selectivity,. The technology described can be readily expanded to other drugs biomolecules and molecular targets and should facilitate the development of PET imaging agents for drug testing.

Supplementary Material

Refer to Web version on PubMed Central for supplementary material.

References

1. Rouleau M, Patel A, Hendzel MJ, Kaufmann SH, Poirier GG. Nat Rev Cancer. 2010; 10:293–301. [PubMed: 20200537]
2. Ratnam K, Low JA. Clin Cancer Res. 2007; 13:1383–1388. [PubMed: 17332279]
3. Comen EA, Robson M. Oncology (Williston Park). 2010; 24:55–62. [PubMed: 20187322]
4. Weissleder R, Pittet MJ. Nature. 2008; 452:580–589. [PubMed: 18385732]
5. Avril N, Rosé CA, Schelling M, Dose J, Kuhn W, Bense S, Weber W, Ziegler S, Graeff H, Schwaiger M. J Clin Oncol. 2000; 18:3495–3502. [PubMed: 11032590]
6. Burns HD, et al. Proc Natl Acad Sci U S A. 2007; 104:9800–9805. [PubMed: 17535893]
7. Gambhir SS. Nat Rev Cancer. 2002; 2:683–693. [PubMed: 12209157]
8. Willmann JK, van Bruggen N, Dinkelborg LM, Gambhir SS. Nat Rev Drug Discov. 2008; 7:591–607. [PubMed: 18591980]
9. Klimas MT. Mol Imaging Biol. 2002; 4:311–337. [PubMed: 14537107]
10. Reiner T, Earley S, Turetsky A, Weissleder R. Chem Bio Chem. 2010 *in print*.
11. Keliher EJ, Reiner T, Turetsky A, Weissleder R. ChemMedChem. 2010 *in print*.
12. Chang PV, Prescher JA, Sletten EM, Baskin JM, Miller IA, Agard NJ, Lo A, Bertozzi CR. Proc Natl Acad Sci U S A. 2010; 107:1821–1826. [PubMed: 20080615]
13. Blackman ML, Royzen M, Fox JM. J Am Chem Soc. 2008; 130:13518–13519. [PubMed: 18798613]
14. Devaraj NK, Upadhyay R, Haun JB, Hilderbrand SA, Weissleder R. Angew Chem Int Ed Engl. 2009; 48:7013–7016. [PubMed: 19697389]
15. Devaraj NK, Hilderbrand S, Upadhyay R, Mazitschek R, Weissleder R. Angew Chem Int Ed Engl. 2010; 49:2869–2872. [PubMed: 20306505]
16. Devaraj NK, Keliher EJ, Thurber GM, Nahrendorf M, Weissleder R. Bioconjug Chem. 2009; 20:397–401. [PubMed: 19138113]
17. Devaraj NK, Weissleder R, Hilderbrand SA. Bioconjug Chem. 2008; 19:2297–2299. [PubMed: 19053305]
18. Haun JB, Devaraj NK, Hilderbrand SA, Lee H, Weissleder R. Nat Nanotechnol. 2010; 5:660–665. [PubMed: 20676091]
19. Ferraris DV. J Med Chem. 2010; 53:4561–4584. [PubMed: 20364863]
20. Menear KA, Adcock C, Boulter R, Cockcroft X-l, Copsey L, Cranston A, Dillon KJ, Drzewiecki J, Garman S, Gomez S, Javaid H, Kerrigan F, Knights C, Lau A, Loh VM Jr, Matthews ITW, Moore S, O'Connor MJ, Smith GCM, Martin NMB. J Med Chem. 2008; 51:6581–6591. [PubMed: 18800822]

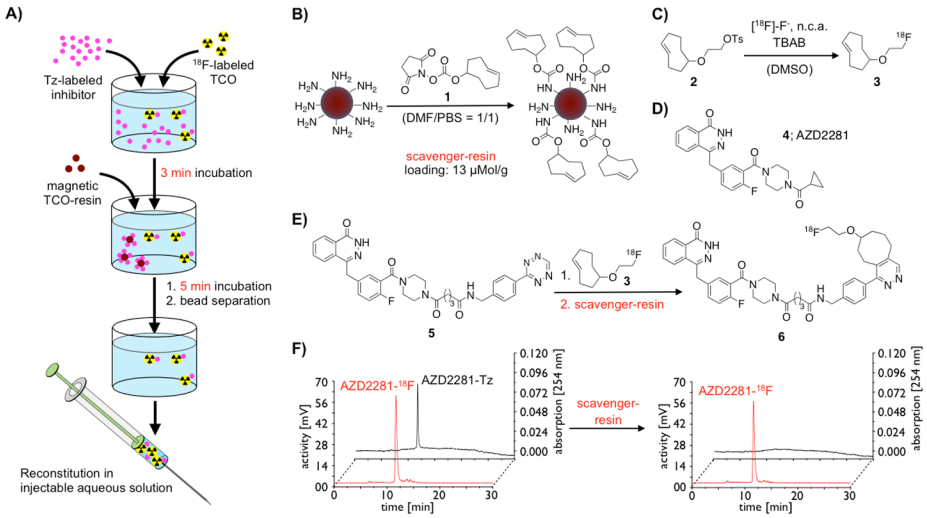

Figure 1.

a) Schematic synthesis of ^{18}F- AZD2281 **6**; ^{18}F-labeled TCO **3** and AZD2281-Tz **5** were combined and incubated for 3 min; Magnetic TCO-scavenger resin was added, incubated for 5 min and removed; Purified ^{18}F- AZD2281 was reconstituted and brought into an injectable volume; b) Synthesis of the magnetic TCO-scavenger resin from amine-decorated beads and NHS-activated TCO **1**; c) synthesis of ^{18}F-labeled TCO; d) Structure of AZD2281 **4**; e) Synthesis and structure of ^{18}F- AZD2281 **6** (only one isomer shown). f) Radioactive and absorption traces of the ^{18}F- AZD2281 reaction mixture before and after purification with the magnetic TCO scavenger resin;

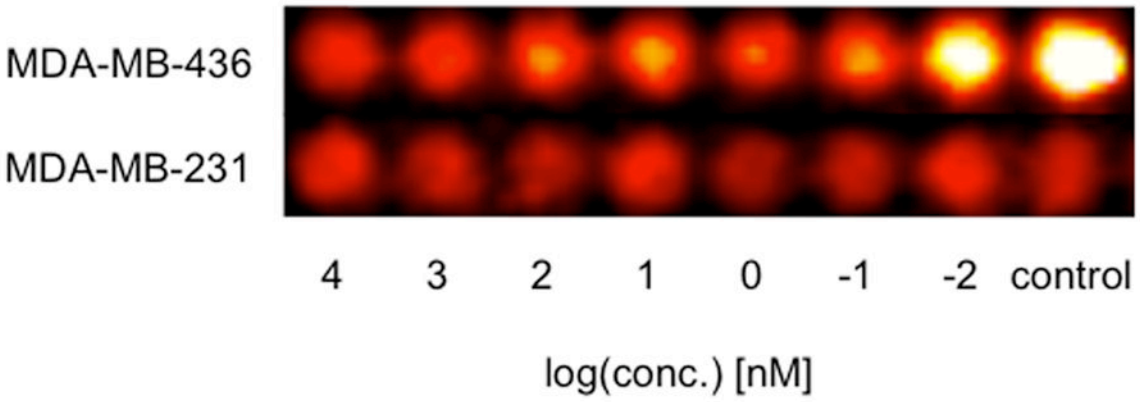

Figure 2.

In vitro competitiv e inhibition essays with F-AZD2281. PARP1-high (MDA-MB-436) and PARP1-low (MDA-MB-231) cells were treated with 5 μCi of ^{18}F- AZD2281 in presence and absence of AZD2281 (10 μM – 0.01 nM). After washing, cell associated activity was determined by gamma-counting. For the control measurement, no AZD2281 was added.

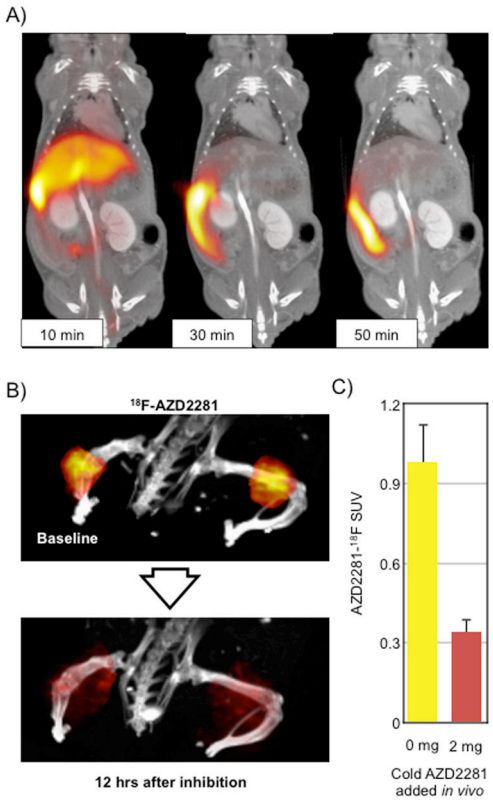

Figure 3.

In vivo evaluation of ^{18}F- AZD2281; a) combined PET/CT scans of a non-tumor bearing mouse injected with ^{18}F-AZD2281 displayed at 10, 30 and 30 minutes post-injection; b) three-dimensional reconstruction of a tumor-bearing animal injected with ^{18}F- AZD2281 with and without pre-injection of AZD2281 (bladder segmented out for clarity); c) quantification of tumor uptake in hind legs with and without pre-injection of AZD2281.